Advanced Frequency Reconfigurable Microstrip Antenna Based on Fractal Geometry for X-Band Applications

Rakesh Kumar Singh[1], Surya Bhushan Dubey[2], Kamal Prakash Pandey[3], Saiyed Salim Sayeed[4], Amrees Pandey[*5]

[1, 5]Department of Electronics and Communication Engineering, Shambhunath Institute of Engineering and Technology (SIET), Prayagraj, Uttar Pradesh, India

[2]Department of Electrical and Electronics Engineering, S. R. Institute of Management and Technology, Lucknow, Uttar Pradesh, India

[3]Department of Electronics and Communication Engineering, BBS College of Engineering and Technology, Prayagraj, Uttar Pradesh, India

[4]Department of Electronics and Communication Engineering, Institute of Technology and Management, Maharajganj, Uttar Pradesh, India

rksingh_rakesh@yahoo.com[1], suryadubey1@gmail.com[2], pandeykamal.1976@gmail.com[3], saiyedsalimsayeed@gmail.com[4], amrishpandey19@gmail.com[5]

[*]**Corresponding Author Email:** amrishpandey19@gmail.com

Abstract: This work presents the design and analysis of a frequency reconfigurable microstrip patch antenna based on fractal geometry for X-band satellite communication. The antenna operates in two switching configurations controlled by a single PIN diode modeled in HFSS. In the OFF state, the antenna covers 8.81–9.65 GHz and 10.28–12.61 GHz, with resonance frequencies at 9.23 GHz, 10.71 GHz, and 11.97 GHz, achieving peak gains of 9.23 dBi, 7.44 dBi, and 11.27 dBi, respectively. In the ON state, the operating bands shift to 8.81–9.44 GHz and 10.07–12.18 GHz, with resonances at 9.23 GHz, 10.71 GHz, and 11.34 GHz, providing peak gains of 6.64 dBi, 10.47 dBi, and 12.23 dBi. The simulated radiation efficiency is 71.19%, 75.63%, and 80.41% in the OFF state, and 72.01%, 78.34%, and 89.68% in the ON state. The inclusion of circular fractal slots in the ground plane significantly enhances bandwidth and gain performance. The findings demonstrate that the proposed fractal reconfigurable antenna offers high radiation efficiency and reliable multi-band operation, making it a strong candidate for X-band wireless and satellite communication applications.

Keywords: PIN Diode Switching, X-Band, Bandwidth Enhancement, VSWR, FRA

1. Introduction

With the continuous advancement in antenna engineering, Fractal Reconfigurable Antennas (FRAs) have emerged as a highly promising research area. The unique attributes of fractals-such as self-similarity, self-affinity, and space-filling properties-when combined with electronic reconfigurability, enable dynamic adjustment of antenna parameters, making FRAs an attractive choice for modern multifunctional antenna systems [1]. Typically, microstrip patch antennas are employed as the basic structure, wherein the integration of fractal geometries and switching mechanisms becomes a key aspect of the design. For instance, reconfigurable annular slot antennas using PIN diodes have been developed to achieve both frequency and radiation pattern reconfigurability [2]. Similarly, triangular patch-based

reconfigurable antennas integrated with UWB antennas have been proposed for cognitive radio applications [3].

Researchers have extensively investigated diverse approaches to design fractal-shaped and reconfigurable antennas in order to meet the growing demands of commercial and satellite communication systems [4–5]. Reconfigurable antennas can generally be categorized into four types: frequency reconfigurable, pattern reconfigurable, polarization reconfigurable, and compound reconfigurable antennas**,** depending on the dynamically adjusted operating parameter [6–7]. Various studies demonstrate that incorporating fractal geometries in reconfigurable antenna designs significantly improves bandwidth, radiation efficiency, and compactness, making them suitable across multiple frequency bands [8–9]. In addition, optimization of switching elements has been explored to reduce the number of components required for reconfiguration, thereby improving reliability and overall performance [10].

The use of PIN diodes as switching elements has been extensively reported to achieve effective frequency reconfigurability [11–14]. Their integration influences several antenna characteristics, including impedance matching, radiation efficiency, and gain, particularly in multiband reconfigurable microstrip patch antennas for next-generation wireless systems [15–16]. Such designs have enabled antennas to switch between ultra-wideband and narrowband modes**,** offering greater adaptability for different applications [17].

In the current wireless communication era, there is a strong demand for antennas that provide multiband characteristics, compactness, and high performance [18]. Antenna selection is often governed by critical factors such as size, weight, bandwidth, gain, design complexity, cost-effectiveness, and suitability for specific applications [19]. Studies on rectangular microstrip patch antennas highlight their potential for broadband operations, while multiband microstrip antennas are widely recognized for their lightweight, low-profile, and multi-frequency capabilities [20–22].

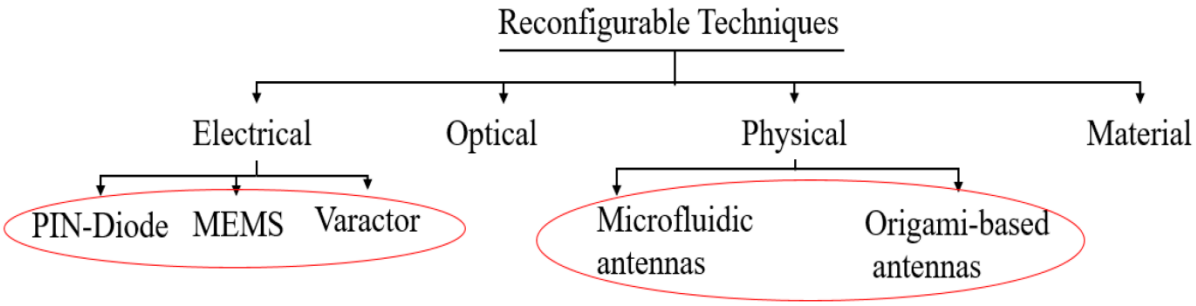

Fig. 1: Representative techniques for designing reconfigurable antennas

Nonetheless, to fully support the requirements of emerging wireless and satellite communication systems, further advancements are essential to enhance bandwidth, radiation efficiency, and reconfigurability in microstrip antenna designs [23].

Varactor diodes and PIN diodes are widely employed in reconfigurable antenna designs due to their fast switching characteristics, and in many cases, they can serve as effective alternatives to RF MEMS devices [24]. Reconfiguration can be achieved using different switching mechanisms, such as PIN diodes, RF MEMS, varactor diodes, lumped elements, or capacitive switches [25]. Among these, PIN diodes are particularly attractive owing to their

fast switching speed, typically ranging from 1 to 100 ns, and their strong capability to dynamically alter antenna characteristics [26–27].

Several studies have reported the use of these switching elements to realize different types of reconfigurable antennas tailored for various wireless communication applications. For example, both frequency and radiation pattern reconfigurability have been demonstrated through the integration of PIN diodes and varactor diodes in antenna structures [28–29].

In this work, the design of the proposed **Fractal Reconfigurable Antenna (FRA)** is presented in a systematic manner, followed by a detailed discussion of the simulation results and performance evaluation.

2. Analysis and Optimization of Fractal Geometry for Reconfigurable Antenna Design

This section describes the fundamental geometry and design methodology of the proposed X-band frequency reconfigurable antenna. Frequency reconfigurability is realized in simulation by employing the lumped RLC equivalent circuit model of the PIN diode. By controlling the diode's ON/OFF switching states, the antenna can operate across different frequency bands. Enhanced radiation efficiency and satisfactory far-field characteristics are achieved through the implementation of a fractal ground plane.

The proposed design has been developed through multiple stages of optimization, as illustrated in Fig. 2 and Fig. 3. Initially, a rectangular FR4 substrate with dimensions 22 × 22 × 1.6 mm³ is used as the antenna base. A conducting rectangular patch of size 14 × 14 mm² is then placed on the substrate. The design of the rectangular patch follows the subsequent procedure. Furthermore, a detailed parametric analysis of the radiating element and ground structure was carried out, governed by the standard design equations (a)–(f) [13–19]. The patch width (W) of the antenna was calculated using the following fundamental expression:

$$\mathrm{W} = \frac{c}{2f}\sqrt{\frac{2}{\varepsilon_{\mathrm{r}+1}}} \tag{a}$$

Where, ε_{r} is the dielectric constant of substrate and f is the center frequency, Length of patch is calculated by the equation:

$$\mathrm{L} = \mathrm{L}_{ef} - 2\Delta\mathrm{l} \tag{b}$$

$$\mathrm{L}_{ef} = \frac{c}{2f\sqrt{\varepsilon_{\mathrm{re}}}} \tag{c}$$

Where L_{ef} is the Patch effective length and $\varepsilon_{\mathrm{re}}$ is the effective substrate dielectric constant is given by;

$$\varepsilon_{\mathrm{re}} = \frac{\varepsilon_{\mathrm{re}}+1}{2} + \frac{\varepsilon_{\mathrm{r}}-1}{2}\left[1+\frac{12h}{\mathrm{W}}\right]^{-1/2} \tag{d}$$

Where, h is the thickness of substrate and the normalized extension in length (Δl) is given by:

$$\Delta l = 0.412\ h \frac{(\varepsilon_{re} + 0.3)\left(\frac{W}{h} + 0.8\right)}{(\varepsilon_{re} - 0.25\ B)\left(\frac{W}{h} + 0.8\right)} \quad \text{(e)}$$

Feed line length (L_f) is considered by using below equation.

$$L_f = \lambda_g/2 \quad \text{(f)}$$

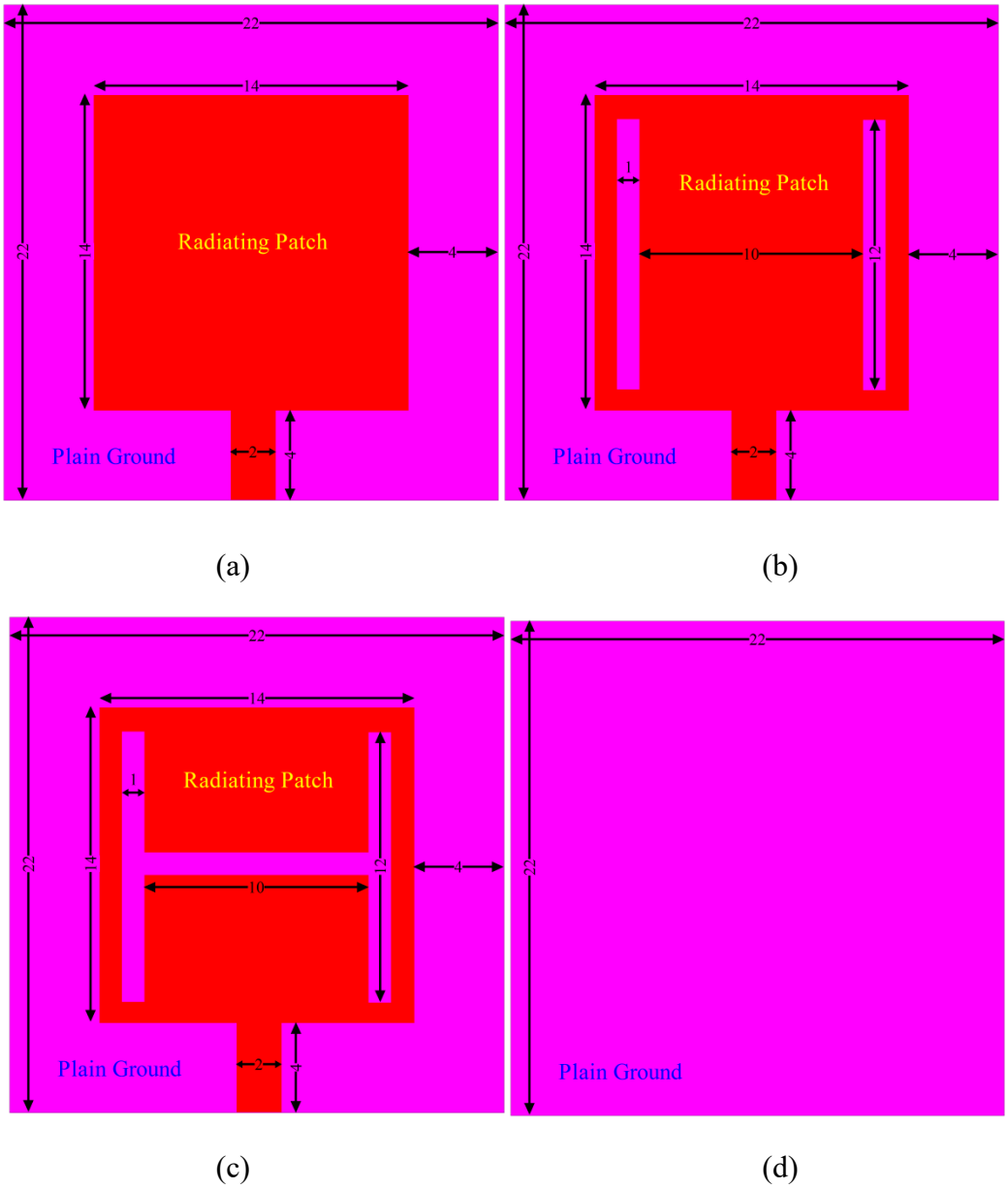

Fig. 2: Evolution stages of the proposed antenna design: (a) A_1, (b) A_2, (c) A_3, and (d) corresponding plain ground structure [Dimensional units: mm].

The radiating patch is optimized by introducing an H-shaped slot etched into the rectangular patch. The position and dimensions of this slot, along with the additional fractal circular slots embedded in the ground plane, are obtained through multiple stages of optimization, as

illustrated in Fig. 1 and Fig. 2. The antenna employs a simple ground structure and is excited using a stripline feed of size 2 × 4 mm².

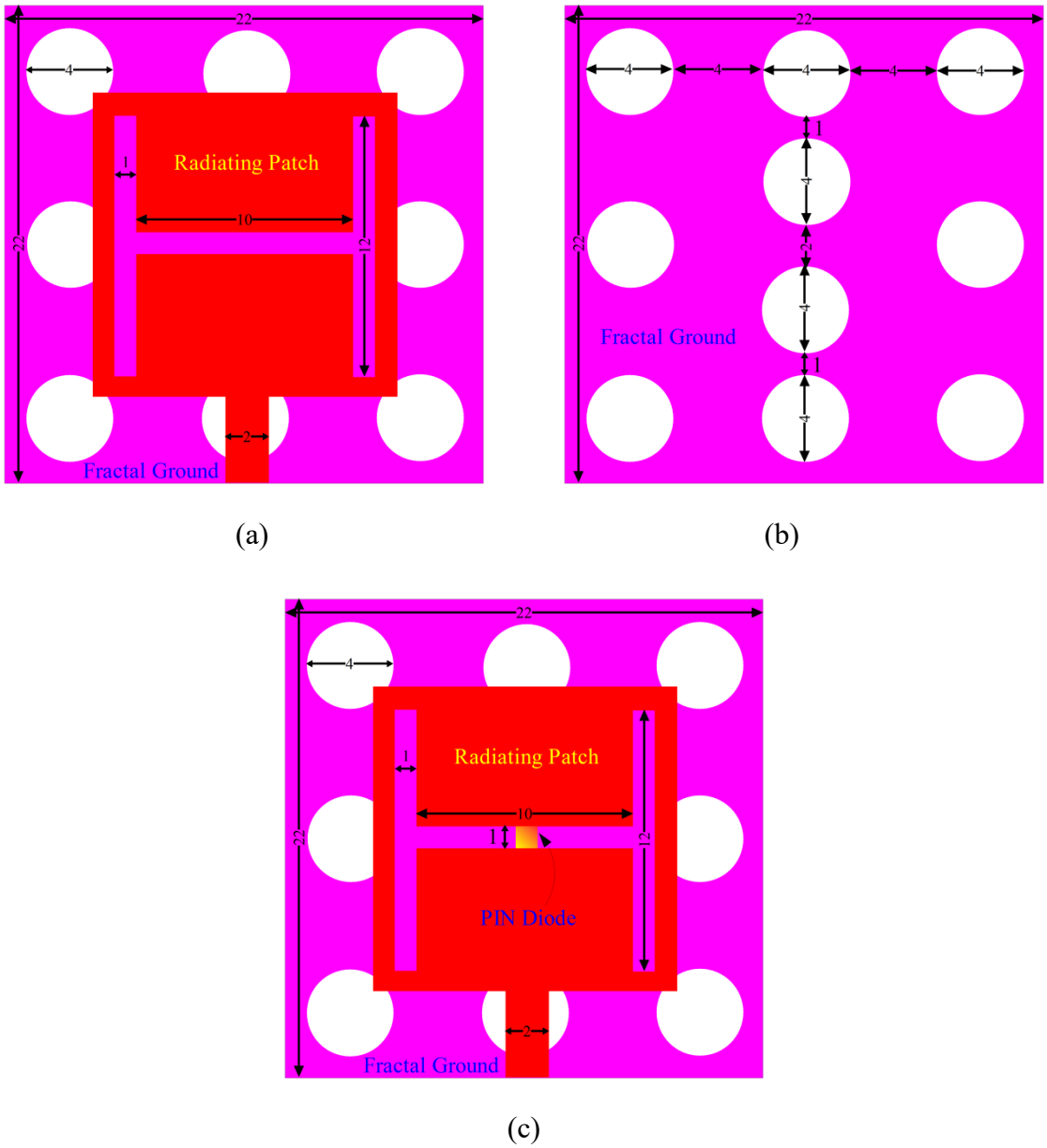

Fig. 3: Evolution of the proposed antenna - (a) A4 structure, (b) Fractal ground of A_4–A_5, and (c) Final A_5 design with diode ON/OFF states [Dimensional units in mm].

Initially, a conventional microstrip patch antenna (Fig. 3) was designed on a low-cost FR4-epoxy substrate with a thickness of 1.6 mm and a relative permittivity of 4.4. The radiating patch is excited using a microstrip-line feed [15], with feed-line dimensions of 4 mm (length) × 2 mm (width). The baseline antenna models A_1–A_3 are maintained with an overall size of 22 × 22 mm², incorporating a plain ground structure, as illustrated in Fig. 2(a–d).

For further improvement, the subsequent designs (A_4–A_5) integrate circular-shaped fractal slots of size 4 × 4 mm² in the ground plane, as depicted in Fig. 3(a–c). The incorporation of these fractal slots leads to significant enhancement in both bandwidth and radiation performance, validating the effectiveness of the proposed optimization methodology.

In Fig. 3(a), the geometry represents the PIN diode in the OFF state, where a 10 × 1 mm slot is etched at the central region of the radiating patch. This configuration satisfies the reconfigurability criteria required for X-band satellite applications. Furthermore, the addition of a parallel rectangular slot (12 × 1 mm) plays a critical role in improving the antenna's gain and operating bandwidth.

The final optimized antenna geometry (A_4–A_5) is developed by modifying the initially designed plain ground with a fractal ground plane, as shown in Fig. 2(a–d) and Fig. 3(a–c). A single PIN diode is employed as the switching element for achieving reconfigurability. It is strategically placed at the center of the rectangular slot etched on the radiating patch, as highlighted in Fig. 3(a).

The geometry shown in Fig. 3(b) illustrates the incorporation of fractal circular slots on the ground plane. For reconfigurability, a surface-mount PIN diode from the Skyworks series (dimension: 1 mm × 1 mm, as specified in the datasheet) is employed and modeled in HFSS [11–14]. The diode is represented using its equivalent RLC network, which accounts for both ON and OFF switching conditions, as shown in Fig. 4.

A single PIN diode is utilized for switching purposes, owing to its ability to behave as a variable resistor in the RF range. Depending on its biasing state, the diode exhibits either open-circuit or short-circuits behavior at the insertion point, thereby altering the effective resonant length of the patch. This variation enables the antenna to reconfigure its operating frequency dynamically.

In the ON state, the diode is modeled as a low-value resistor (R_L = 1.5 Ω) in series with an inductor (L = 0.7 nH), forming an RL equivalent circuit. Conversely, in the OFF state, it is represented as a parallel configuration of a high-value resistor (R_h) and a capacitor (C = 0.15 pF) with an inductor (L = 0.7 nH), thus behaving as an RLC circuit. The accurate modeling of the Skyworks PIN diode in HFSS ensures realistic simulation of the antenna's reconfigurable characteristics.

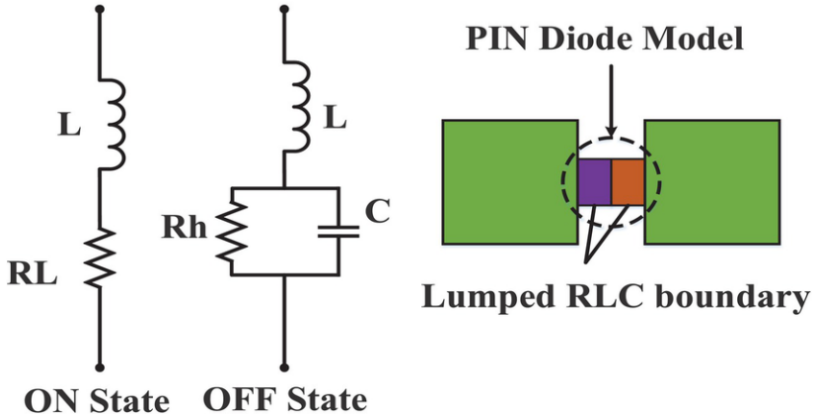

Fig. 4: Equivalent circuit representation of the PIN diode in ON and OFF states for reconfigurable antenna operation.

3. Results and Interpretations

The proposed antenna structure was modeled and analyzed using the High-Frequency Structure Simulator (HFSS). Key performance parameters, such as return loss, gain, and radiation characteristics, were carefully evaluated. During the simulation process, it was

observed that employing a discrete frequency sweep provides higher accuracy compared to a continuous sweep, as it computes the solution at each selected frequency point rather than interpolating the intermediate values. This approach not only enhances the precision of the simulated results but also significantly reduces computational time and memory requirements. The subsequent analysis focuses on the antenna's performance metrics and radiation behavior, thereby validating the effectiveness of the proposed design for X-band applications.

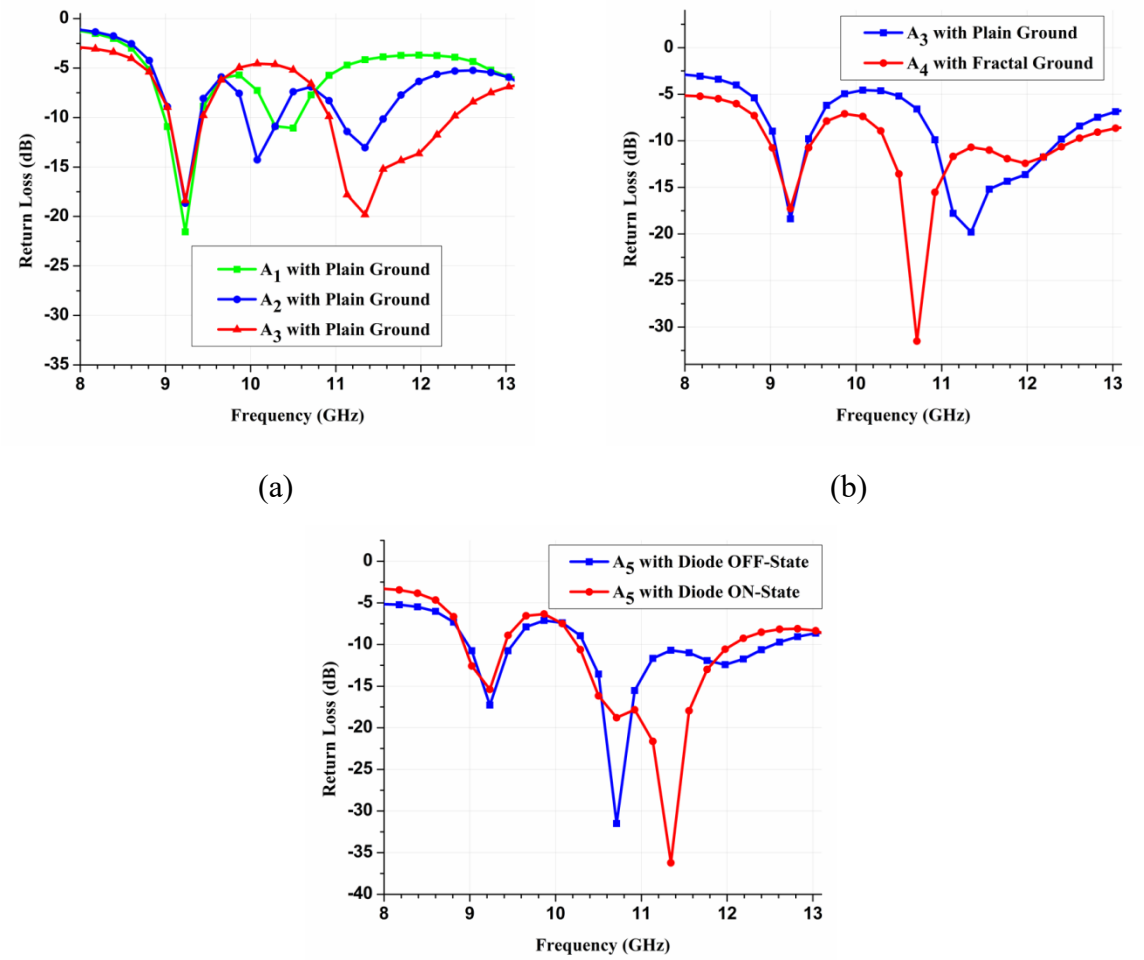

(a) (b)

(c)

Fig. 5: Simulated return loss (S_{11}) characteristics as a function of frequency for different antenna configurations: (a) conventional designs A_1–A_3, (b) intermediate optimized design A_3–A_4, and (c) the final proposed reconfigurable antenna (A_5).

The performance of the proposed antenna, in terms of return loss (dB) and peak gain, is illustrated in Fig. 5(a–c) and Fig. 6(a–c), while the summarized numerical results for antenna configurations A_1–A_5 are tabulated in Table 1.

For the initial configuration (A_1), the simulated return loss response, shown in Fig. 5(a), indicates two operating bands at 8.81–9.44 GHz and 10.07–10.71 GHz, resonating at 9.23 GHz and 10.50 GHz, respectively. However, the corresponding gain values (Fig. 6(a)) were found to be relatively poor, with peak values of -0.30 dBi and -2.04 dBi, indicating insufficient radiation performance.

To overcome this limitation, two parallel rectangular slots of dimension 12 × 1 mm² were etched onto the radiating patch, leading to the improved configuration (A_2). As a result, the antenna demonstrated significant enhancement in radiation performance. The modified design yielded three operating bands at 9.02–9.44 GHz, 9.86–10.50 GHz, and 10.92–11.76 GHz, with resonances at 9.23 GHz, 10.07 GHz, and 11.34 GHz, respectively. Correspondingly, the peak gains were substantially improved to 2.39 dBi, -0.97 dBi, and 4.92 dBi, as compared to the negative gain values observed in A1.

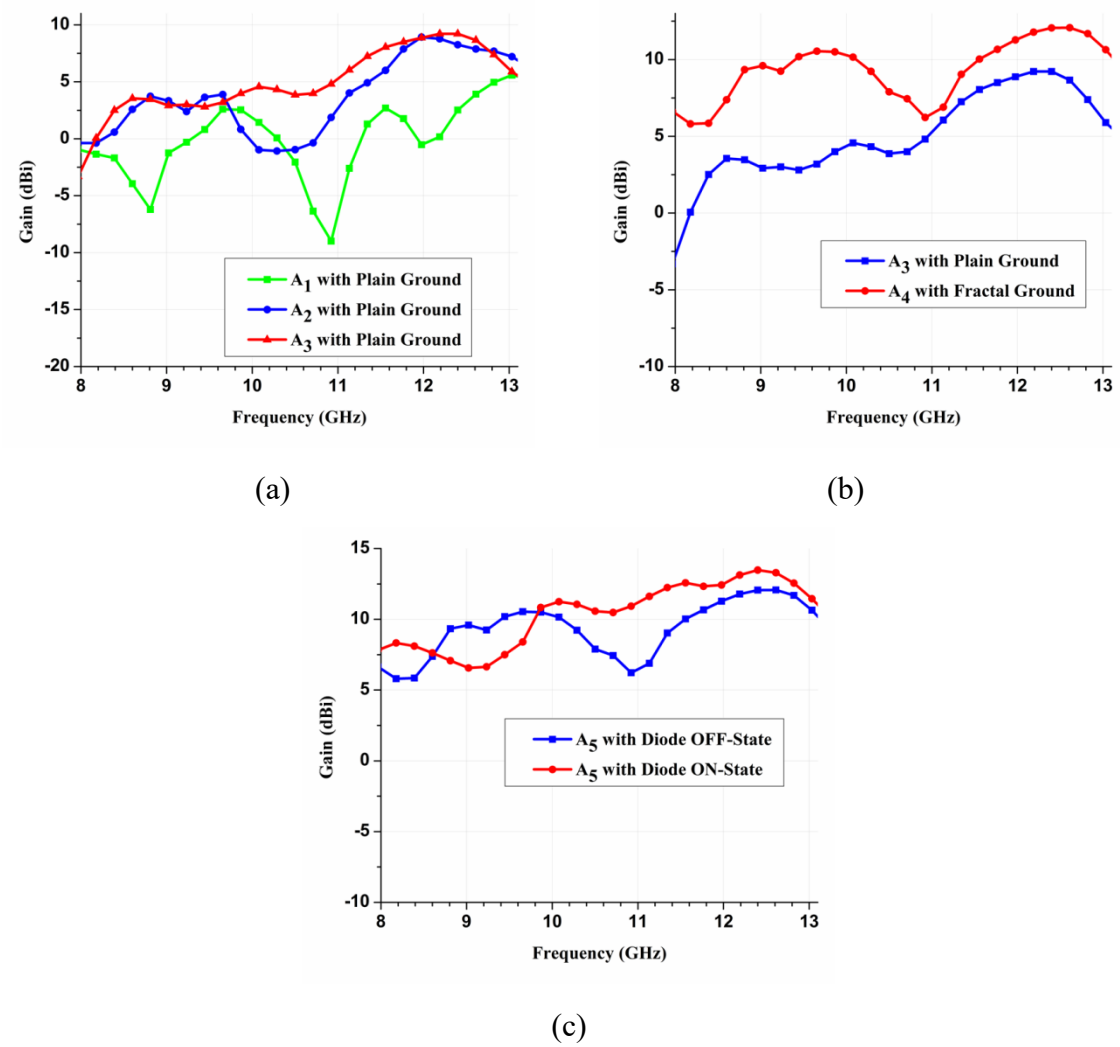

Fig. 6: Gain variation with frequency for different antenna stages: (a) A_1–A_3, (b) A_3 vs. A_4 with fractal ground, and (c) proposed A_5 under diode ON/OFF states.

After analyzing the performance of A_2, it was observed that both gain and bandwidth required further improvement. To achieve this, an additional rectangular slot of 10 × 1 mm² was etched at the mid-section of the radiating patch, leading to the design of A_3. The resulting antenna provided dual operating bands of 9.02–9.44 GHz and 10.92–12.40 GHz, resonating at 9.23 GHz and 11.34 GHz, with peak gains of 3.06 dBi and 7.24 dBi, respectively. Compared to A_1, the performance of A3 showed a significant enhancement in both gain and bandwidth.

Figures 5(b) and 6(b) illustrate the return loss and gain characteristics of A_3 and A_4, respectively. While A_3 employed a conventional plain ground, A_4 was developed using a fractal ground plane structure. The A4 configuration exhibited dual operating bands of 8.81–9.65 GHz and 10.28–12.61 GHz, resonating at 9.23 GHz, 10.71 GHz, and 11.97 GHz, with peak gains of 9.23 dBi, 7.44 dBi, and 11.27 dBi, respectively. These results clearly demonstrate that the integration of a fractal ground structure in A_4 yields a substantial improvement in both bandwidth and gain compared to A_3.

Figures 5(c) and 6(c) depict the return loss and gain responses of the final proposed design, A_5, under diode OFF and ON switching states. In the OFF state, the A_5 structure exhibits a performance nearly identical to A_4. However, when the diode is switched ON, the antenna resonates over two wide operating bands of 8.81–9.44 GHz and 10.07–12.18 GHz, with resonant frequencies at 9.23 GHz, 10.71 GHz, and 11.34 GHz, achieving peak gains of 6.64 dBi, 10.47 dBi, and 12.23 dBi, respectively.

Importantly, the reconfiguration achieved by the PIN diode allows the antenna to dynamically switch between different frequencies bands, thereby enabling its use in multiple wireless and X-band satellite applications. In both ON and OFF states, the S11 parameter remains well below -10 dB, validating excellent impedance matching and efficient radiation performance.

Table 1: Performance Characteristics of Antenna Design Configurations (A1-A5)

Design Configuration	Operating Band (GHz)	Resonant Frequency (GHz)	Return Loss (dB)	Peak Gain (dBi)	Radiation Efficiency (%)	VSWR
A_1	08.81-09.44	09.23	-21.55	-0.30	76.72	1.43
	10.07-10.71	10.50	-11.06	-2.04	74.23	1.76
A_2	09.02-09.44	09.23	-18.65	2.39	80.33	1.22
	09.86-10.50	10.07	-14.27	-0.97	77.48	1.59
	10.92-11.76	11.34	-13.03	04.92	72.21	0.48
A_3	09.02-09.44	09.23	-18.38	03.06	81.13	1.24
	10.92-12.40	11.34	-19.80	07.24	72.41	0.65
A_4	08.81-09.65	09.23	-17.27	09.23	71.19	1.31
	10.28-12.61	10.71	-31.50	07.44	75.63	0.41
		11.97	-12.41	11.27	80.41	1.87
A_5	08.81-09.44	09.23	-15.39	06.64	72.01	1.65
	10.07-12.18	10.71	-18.78	10.47	78.34	1.82
		11.34	-36.22	12.23	89.68	1.32

Fig. 7(a) illustrates the radiation efficiency performance of antenna A3 with plain ground and A4 with fractal ground geometry, while Fig. 7(b) depicts the efficiency variation under ON and OFF states of the PIN diode in the proposed reconfigurable antenna (A_5). Across all operating frequency bands, the radiation efficiency remains consistently above 70%, which indicates a highly effective radiation mechanism. Such high efficiency confirms the antenna's suitability for reliable wireless communication applications.

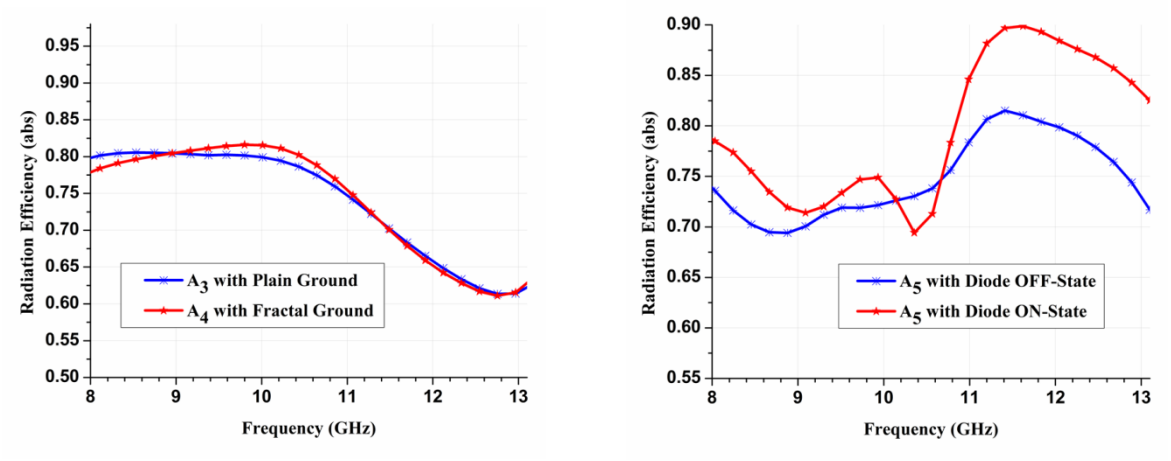

(a) (b)

Fig. 7: Variation of radiation efficiency with frequency for different antenna configurations: (a) Comparison between A_3 with plain ground and A_4 with fractal ground geometry, and (b) radiation efficiency response of the proposed reconfigurable antenna (A_5) under PIN diode ON and OFF switching conditions.

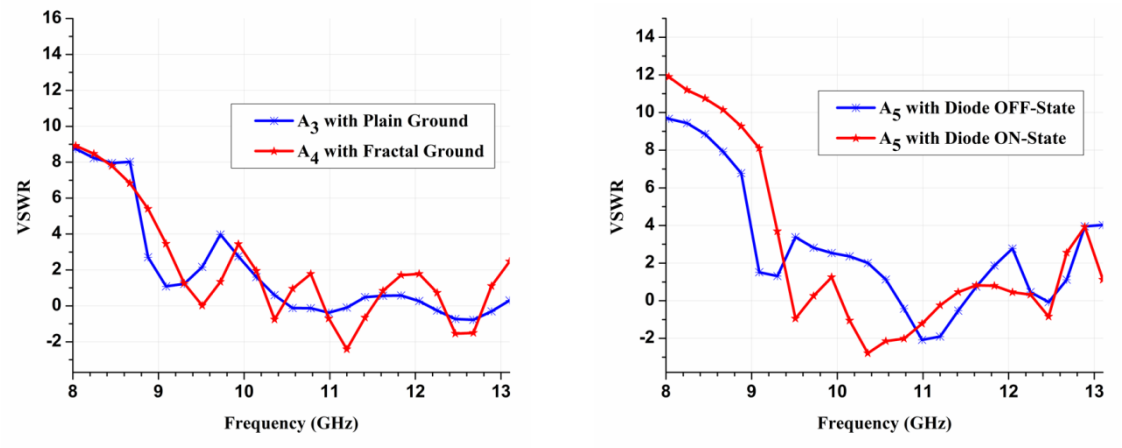

(a) (b)

Fig. 8: Variation of VSWR with frequency for different antenna configurations: (a) Comparison of A_3 with plain ground and A_4 with fractal ground geometry, and (b) VSWR characteristics of the proposed reconfigurable antenna (A_5) under PIN diode ON and OFF switching states.

Similarly, Fig. 8(a) shows the Voltage Standing Wave Ratio (VSWR) characteristics of antenna A_3 and A_4, highlighting the improvement achieved through the implementation of fractal ground geometry. Fig. 8(b) further demonstrates the VSWR response of the proposed reconfigurable antenna (A_5) under diode ON and OFF states. In both switching conditions, the VSWR values are observed to remain well below 2 at all resonant frequencies, ensuring good impedance matching and stable performance.

The proposed antenna achieves a maximum gain of 12.23 dBi at 11.34 GHz, confirming its strong directional capability. Furthermore, the performance parameters, including resonant frequencies, return loss, gain, efficiency, and VSWR, as summarized in Table 1, show

consistent agreement across all design configurations. This consistency validates the robustness of the proposed design evolution and highlights the effectiveness of the reconfigurable antenna for advanced wireless and satellite communication systems.

The E-field and H-field radiation patterns of the proposed frequency reconfigurable antenna (FRA) were analyzed at the respective resonant frequencies for φ = 0° and φ = 90°, as illustrated in Fig. 9(a–f). The results confirm that the proposed antenna exhibits stable and consistent radiation characteristics under both ON and OFF states of the PIN diode. In each case, the main lobe maintains the maximum radiation, ensuring effective directional performance.

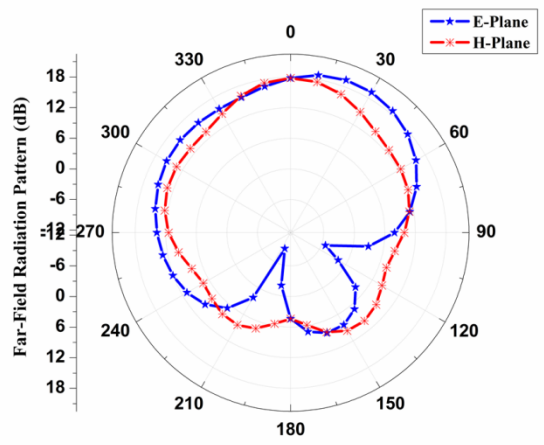

(a)

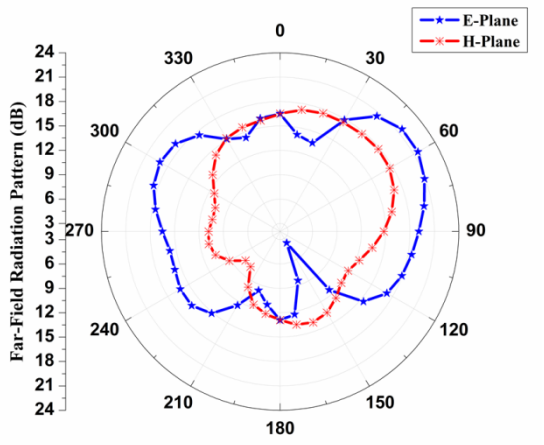

(b)

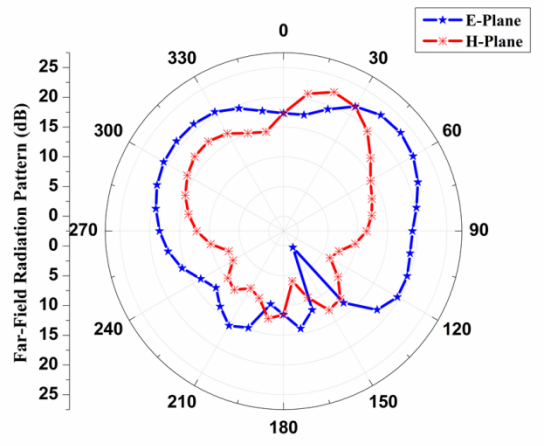

(c)

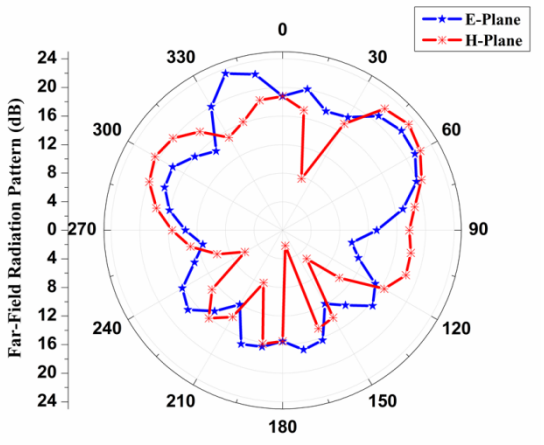

(d)

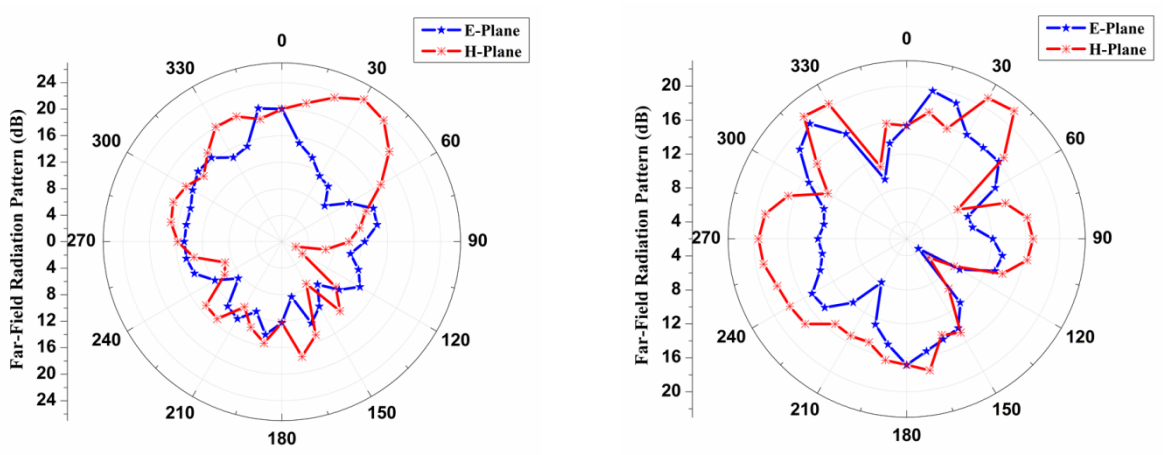

(e) (f)

Fig. 9: Simulated E- and H-plane radiation patterns of the proposed antenna under diode switching conditions: (a-c) OFF state at 9.23, 10.71, and 11.97 GHz, and (d-f) ON state at 9.23, 10.71, and 11.34 GHz, demonstrating stable and directional radiation behavior.

Specifically, Fig. 9(a–c) illustrates the radiation patterns under the OFF-state diode condition, corresponding to resonant frequencies at 9.23 GHz, 10.71 GHz, and 11.97 GHz, respectively. Similarly, Fig. 9(d–f) presents the patterns under the ON-state diode condition, resonating at 9.23 GHz, 10.71 GHz, and 11.34 GHz. Across all observed cases, the antenna maintains a directional and stable far-field pattern, demonstrating effective frequency reconfigurability while preserving radiation stability.

The simulated results confirm that the proposed FRA achieves high gain, stable radiation lobes, and reliable directivity across multiple frequency bands, making it highly suitable for diverse wireless communication applications.

Table 2: Comparative analysis of the proposed reconfigurable antenna with reported designs

Ref.	Dimensions (mm^3)	Operating Band (GHz)	Peak Gain (dBi)	VSWR	Radiation Efficiency (%)
[14]	60×60×0.8	07.32-08.23	3.72	NR	69.50
[15]	45×45×1.6	10.21-11.85	2.45	NR	72
[16]	40×40×1.57	05.72-07.12	2.75	1.80	NR
[18]	35×35×1.6	08.63-09.25 10.44-11.42	2.78 1.50	NR	62.58
[21]	28×28×1.6	12.86-13.58	2.98	NR	NR
[22]	39×37×1.6	13.64-14.62	3.86	2	NR
Proposed	22×22×1.6	08.81-09.44 10.07-12.18	6.64 10.47 12.23	1.32-1.82	72.01-89.68

The proposed antenna has been compared with several previously reported works that incorporate reconfigurability into fractal antenna designs. The comparative analysis, as presented in Table 2, highlights that the proposed design offers significant advantages in terms of compactness, low profile, and conformability. It demonstrates excellent impedance matching, high radiation efficiency, stable and directional radiation patterns, acceptable gain performance, and VSWR values consistently below the desired threshold. Furthermore, the proposed antenna provides reliable frequency reconfigurability, making it highly suitable for modern wireless communication systems. Overall, the design exhibits promising performance, particularly for X-band satellite communication applications, thereby validating its effectiveness and practical applicability.

4. Conclusion

This paper presents the design and analysis of a novel fractal and frequency-reconfigurable microstrip patch antenna, where reconfigurability is achieved through the integration of a PIN diode. The simulation results demonstrate that the adoption of fractal geometry significantly enhances the impedance bandwidth and gain performance, while the inclusion of the PIN diode introduces frequency reconfigurability, enabling the antenna to operate at three distinct resonant frequencies under different switching states (ON/OFF conditions). By combining the advantages of both fractal geometries and reconfigurable antenna techniques, the proposed design successfully delivers superior performance in terms of gain, bandwidth, and radiation characteristics.

Moreover, the antenna exhibits a compact size, low profile, lightweight structure, and stable radiation patterns, making it well-suited for practical deployment in modern communication systems. The achieved performance parameters validate the antenna's applicability for X-band satellite communication systems, as well as for other wireless applications that demand frequency agility, high efficiency, and reliable operation. The proposed design thus represents a promising solution for next-generation wireless and satellite communication devices.

References

[1] P. Thanki and F. Raval, "I-shaped frequency and pattern reconfigurable antenna for WiMAX and WLAN applications," *Progress in Electromagnetics Research Letters*, vol. 97, pp. 149–156, 2021.

[2] A. K. Saroj and J. A. Ansari, "A reconfigurable multiband rhombic shaped microstrip antenna for wireless smart applications," *International Journal of RF and Microwave Computer-Aided Engineering*, vol. 30, p. e22378, Oct. 2020.

[3] M. Ikram, N. Nguyen-Trong, and A. Abbosh, "A simple single-layered continuous frequency and polarization-reconfigurable patch antenna array," *IEEE Transactions on Antennas and Propagation*, vol. 68, no. 6, pp. 4991–4996, 2019.

[4] S. Xiao, B. Z. Wang, and X. S. Yang, "A novel frequency-reconfigurable patch antenna," *Microwave and Optical Technology Letters*, vol. 36, no. 4, pp. 295–297, 2003.

[5] H. T. Chattha, M. Hanif, X. Yang, I. E. Rana, and Q. H. Abbasi, "Frequency reconfigurable patch antenna for 4G LTE applications," *Progress in Electromagnetics Research M*, vol. 69, pp. 1–13, 2018.

[6] A. Tirunagari, B. Madhav, C. V. Kumar, P. Sruthi, M. Sahithi, and K. V. Manikanta, "Design of a frequency reconfigurable fractal antenna for Internet of Things (IoT) in vehicular communication," *International Journal of Recent Technology and Engineering*, vol. 7, pp. 1605–1611, 2019.

[7] W. I. Roseli, N. H. Moktar, and M. T. Ali, "Polarization reconfigurable microstrip patch antenna for wireless communication applications," in *Proc. Int. Symp. Antennas Propag. (ISAP)*, Busan, Korea (South), 2018, pp. 1–2.

[8] M. Saravanan and M. J. S. Rangachar, "Polarization reconfigurable square patch antenna for wireless communications," *Advanced Electromagnetics*, vol. 7, no. 4, pp. 103–108, 2018.

[9] R. K. Singh, A. Basu, and S. K. Koul, "Reconfigurable microstrip patch antenna with polarization switching in three switchable frequency bands," *IEEE Access*, vol. 8, pp. 119376–119386, 2020.

[10] J. Kumar, B. Basu, and F. A. Talukdar, "Modeling of a PIN diode RF switch for reconfigurable antenna application," *Scientia Iranica*, 2018.

[11] X. Zhang, X. Zou, X. Lu, C. W. Tang, and K. M. Lau, "Fully- and quasi-vertical GaN-on-Si PIN diodes: High performance and comprehensive comparison," *IEEE Transactions on Electron Devices*, vol. 64, no. 3, pp. 809–815, 2017.

[12] M. Borhani, P. Rezaei, and A. Valizade, "Design of a reconfigurable miniaturized microstrip antenna for switchable multiband systems," *IEEE Antennas and Wireless Propagation Letters*, vol. 15, pp. 822–825, Sep. 2015.

[13] L. Han, C. Wang, X. Chen, and W. Zhang, "Compact frequency-reconfigurable slot antenna for wireless applications," *IEEE Antennas and Wireless Propagation Letters*, vol. 15, pp. 1795–1798, Mar. 2016.

[14] L. Han, C. Wang, W. Zhang, R. Ma, and Q. Zeng, "Design of frequency- and pattern-reconfigurable wideband slot antenna," *International Journal of Antennas and Propagation*, vol. 2018, pp. 1687–5877, Feb. 2018.

[15] H. F. Abutarboush and A. Shamim, "A reconfigurable inkjet-printed antenna on paper substrate for wireless applications," *IEEE Antennas and Wireless Propagation Letters*, vol. 17, pp. 1648–1651, Jul. 2018.

[16] H. Dholakiya, D. Pujara, and S. B. Sharma, "Wide-slot fractal antenna design with improved bandwidth," in *Proc. IEEE Applied Electromagnetics Conf. (AEMC)*, 2011, pp. 1–3.

[17] W. Chen, G. Wang, and C. Zhang, "Small-size microstrip patch antennas combining Koch and Sierpinski fractal shapes," *IEEE Antennas and Wireless Propagation Letters*, vol. 7, pp. 738–741, 2008.

[18] H. Oraizi and S. Hedayati, "Miniaturized UWB monopole microstrip antenna design by the combination of Giuseppe Peano and Sierpinski carpet fractals," *IEEE Antennas and Wireless Propagation Letters*, vol. 10, pp. 67–70, 2011.

[19] Y. Cai, K. Li, Y. Yin, S. Gao, W. Hu, and L. Zhao, "A low-profile frequency reconfigurable grid-slotted patch antenna," *IEEE Access*, vol. 6, pp. 36305–36312, 2018.

[20] H. A. Majid, M. K. Abdul Rahim, M. R. Hamid, N. A. Murad, and M. F. Ismail, "Frequency-reconfigurable microstrip patch-slot antenna," *IEEE Antennas and Wireless Propagation Letters*, vol. 12, pp. 218–220, 2013.

[21] H. Gu, J. Wang, L. Ge, and C. Sim, "A new quadri-polarization reconfigurable circular patch antenna," *IEEE Access*, vol. 4, pp. 4646–4651, 2016.

[22] W. Li, Y. M. Wang, Y. Hei, B. Li, and X. Shi, "A compact low-profile reconfigurable metasurface antenna with polarization and pattern diversities," *IEEE Antennas and Wireless Propagation Letters*, vol. 20, no. 7, pp. 1170–1174, Jul. 2021.

[23] J. T. Rayno and S. K. Sharma, "Frequency reconfigurable Spirograph planar monopole antenna (SPMA)," in *Proc. Int. Symp. Antennas Propag. (ISAP)*, Nagoya, 2012, pp. 1305–1308.

[24] S. Nikolaou et al., "Pattern and frequency reconfigurable annular slot antenna using PIN diodes," *IEEE Transactions on Antennas and Propagation*, vol. 54, no. 2, pp. 439–448, 2006.

[25] Y. Tawk and C. G. Christodoulou, "A new reconfigurable antenna design for cognitive radio," *IEEE Antennas and Wireless Propagation Letters*, vol. 8, pp. 1378–1381, 2009.

[26] H. C. Mohanta, A. Z. Kouzani, and S. K. Mandal, "Reconfigurable antennas and their applications," *Universal Journal of Electrical and Electronic Engineering*, vol. 6, no. 4, pp. 239–258, 2019.

[27] P. Kaur, A. De, and S. K. Aggarwal, "Design of a novel reconfigurable fractal antenna for multi-band application," *International Journal of Advanced Science and Technology*, vol. 62, pp. 103–112, 2014.

[28] S. Srivastava, P. Mishra, and R. K. Singh, "Design of a reconfigurable antenna with fractal geometry," in *Proc. IEEE UP Section Conf. Electrical, Computer and Electronics (UPCON)*, Allahabad, 2015, pp. 1–6.

[29] J. T. Rayno and S. K. Sharma, "Frequency reconfigurable Spirograph planar monopole antenna (SPMA)," in *Proc. Int. Symp. Antennas Propag. (ISAP)*, Nagoya, 2012, pp. 1305–1308.